HHS Public Access

Author manuscript

Mol Cancer Ther. Author manuscript; available in PMC 2020 March 01.

Published in final edited form as:

Mol Cancer Ther. 2019 March ; 18(3): 507–516. doi:10.1158/1535-7163.MCT-18-0819.

Maternal Embryonic Leucine Zipper Kinase (MELK), a Potential Therapeutic Target for Neuroblastoma

Alexandre Chlenski[1], **Chanyoung Park**[2], **Marija Dobratic**[1], **Helen R. Salwen**[1], **Brian Budke**[2], **Jae-Hyun Park**[3], **Ryan Miller**[1], **Mark A. Applebaum**[1], **Emma Wilkinson**[1], **Yusuke Nakamura**[3,4], **Philip P. Connell**[2], and **Susan L. Cohn**[1]

[1]Department of Pediatrics, University of Chicago, Chicago, IL, USA.

[2]Department of Radiation and Cellular Oncology, University of Chicago, Chicago, IL, USA.

[3]Department of Medicine, University of Chicago, Chicago, IL, USA.

[4]Department of Surgery, University of Chicago, Chicago, IL, USA.

Abstract

Maternal Embryonic Leucine Zipper Kinase (MELK) activates pathways that mediate aggressive tumor growth and therapy resistance in many types of adult cancers. Pharmacologic and genomic inhibition of MELK impairs tumor growth and increases sensitivity to radiation and chemotherapy. Based on these promising preclinical studies, early phase adult clinical trials testing the MELK inhibitor OTS167 are ongoing. To investigate if MELK is also a therapeutic target in neuroblastoma, we analyzed MELK expression in primary tumors and cell lines, and examined the effects of OTS167 on neuroblastoma growth. In primary tumors, high levels of MELK were associated with advanced stage disease and inferior survival. Higher levels of MELK were also detected in tumorigenic versus non-tumorigenic neuroblastoma cell lines, and cells with higher levels of MELK expression were more sensitive to OTS167 than low-MELK expressing cells. OTS167 suppressed the growth of neuroblastoma xenografts, and in a preclinical model of Minimal Residual Disease (MRD), survival was prolonged with MELK inhibition. OTS167 treatment down-regulated MELK and its target Enhancer of Zeste Homolog 2 EZH2, a component of the Polycomb Repressive Complex 2 (PRC2) that is known to modulate the DNA damage response. We also show that OTS167 reduced the formation of collapsed replication forks induced by camptothecin or radiation. Taken together, our results indicate that MELK indirectly mediates efficient processing of replication-associated DNA lesions in neuroblastoma, and that OTS167 sensitizes cells to DNA damaging agents by abrogating this process. Further studies evaluating the activity of combination treatment regimens with OTS167 in neuroblastoma are warranted.

Keywords

MELK; OTS167; neuroblastoma; drug resistance; EZH2

Corresponding author: Susan L. Cohn, Department of Pediatrics, University of Chicago, KCBD Rm. 5100, 900 E. 57th Street, Chicago, IL 60637. scohn@peds.bsd.uchicago.edu.

Conflict of interest: Y. Nakamura is a stockholder and an advisor to OncoTherapy Science, Inc., J-H. Park is a scientific advisor to OncoTherapy Science, Inc. Other authors disclose no potential conflict of interests.

INTRODUCTION

Neuroblastoma is a clinically heterogeneous pediatric cancer. In a subset of patients, the tumors will undergo spontaneous remission without any treatment, and children classified as low- or intermediate-risk (1) are readily cured with surgery with or without adjuvant chemotherapy. However, outcome for patients classified as high-risk remains poor, with survival rates of <50% despite intensive multi-modality therapy (1). Further, survivors of high-risk neuroblastoma are at risk for significant treatment-related late effects (2). Thus, there is an urgent need to identify neuroblastoma vulnerabilities that can be targeted with new therapies that will be more effective and less toxic than our current strategies.

Maternal Embryonic Leucine Zipper Kinase (MELK), a member of the AMP protein kinase (AMPK) family of serine/threonine kinases (3), activates multiple cellular pathways that drive oncogenic growth (4). High levels of MELK are detected in many types of adult solid tumors and leukemia, and increased levels of MELK expression correlate with clinically aggressive disease and poor survival. Further, genomic or pharmacologic inhibition of MELK has been shown to suppress tumor growth *in vitro* and in preclinical adult cancer models (3,5–8), indicating that this kinase is a therapeutic target. A number of studies have shown that MELK inhibition also increases sensitivity to radiation and chemotherapy in preclinical adult cancer models, suggesting that combination treatments may also be effective strategies (3,9–11).

Although the mechanisms by which MELK mediates aggressive tumor growth are not completely understood, MELK has been shown to bind and phosphorylate Forkhead Box Protein M1 (FoxM1) (12). The activated MELK-FoxM1 complex directly binds to the promoter region of Enhancer of Zeste Homolog 2 (EZH2) gene and induces transcription (11). Up-regulation of EZH2, a lysine methyltransferase that catalyzes trimethylation of histone 3 at lysine 27 (H3K27me3), leads to the transcriptional repression of differentiation genes and maintains stem-like properties of cells. MELK-mediated EZH2 activity has also been shown to confer resistance to radiation in several adult cancer models (10,11).

OTS167 is a potent small molecule inhibitor of MELK (13). Nanomolar concentrations of OTS167 efficiently inhibit the proliferation of cancer cells that express high levels of MELK in many types of adult solid tumors (5,6,8,13,14) as well as acute myeloid leukemia (7) and multiple myeloma (15). The drug, however, has little effect on cancer cells with low MELK expression (8,13) or normal cells (15–18). Based on these promising studies, several adult cancer Phase I studies testing OTS167 are currently being conducted (19).

Little is known about the role of MELK in the pathogenesis of pediatric cancers. However, Guan and colleagues have reported that MELK expression is significantly correlated to poor overall survival in patients with neuroblastoma. These investigators also showed that MYCN regulates MELK expression, and that the growth of neuroblastoma xenografts was suppressed with MELK inhibition (18). In this study, we confirmed the prognostic relevance of the level of MELK expression in an expanded cohort of neuroblastoma patients. We also analyzed the correlations between MELK expression, tumor cell phenotype, and response to OTS167 in 11 well-characterized neuroblastoma cell lines with or without MYCN

amplification. In addition, we investigated the anti-tumor activity of OTS167 in preclinical neuroblastoma models, and conducted combination studies with OTS167 to test for synergy with radiation or chemotherapy.

MATERIALS AND METHODS

Cell culture

Neuroblastoma cell lines SK-N-DZ, LA1–55n, SH-SY5Y, NMB, SK-N-BE2, LAN-5, SMS-KCNR, NBL-W-N, NBL-W-S, LA1–5s, and SHEP were grown at 5% CO_2 in RPMI 1640 (Life Technologies) supplemented with 10% heat-inactivated FBS, 2 mM L-glutamine, and 1% penicillin/streptomycin. NBL-W-N, and NBL-W-S were established in our laboratory (20,21), SK-N-DZ was purchased from ATCC, SMS-KCNR was a kind gift from Dr. Carol Thiele, LA1–55n, LA1–5s, SK-N-BE2, SHEP and SH-SY5Y were kind gifts from Dr. June Biedler. All cell lines were authenticated by short tandem repeat profiling and were identical to reference profiles. SK-N-DZ and SK-N-BE2 were authenticated at ATCC using the PowerPlex 18D System (Promega), authentication of LA1–55n, SMS-KCNR, NBL-W-N, NBL-W-S, LA1–5s, and SHEP was performed at The Johns Hopkins University Fragment Analysis Facility (Baltimore, MD) using the AmpFlSTR Identifiler PCR Amplification Kit (Applied Biosystems). All cell lines tested negative for mycoplasma contamination using the MycoAlert detection assay (Lonza).

RNA isolation and quantitative real-time PCR (qPCR)

RNA was isolated using Trizol reagent (Life Technologies), and concentration was determined using UV spectroscopy (DeNovix). Reverse transcription was performed using Superscript III (Life Technologies) according to the manufacturer's instructions. RNA qPCR reactions were set up with 1X Power SYBR Green Master Mix (Applied Biosystems) and 250 nM forward and reverse primers in a 20 ul reaction in a 96-well format. Real-time fluorescent detection of PCR products was performed in a 7500Fast Real-Time PCR System (Applied Biosystems) with 1 cycle at 95°C for 10 minutes; 40 cycles of 95°C for 15 seconds and 60°C for 1 minutes. Pre-made qPCR primer set Hs.PT.58.40892603 targeting exons 10–11 of MELK were purchased from IDT. Primers for GAPDH, which was used as an endogenous control, were described previously (22). Relative quantities of mRNA expression were determined using the comparative ΔΔCt method.

Cell proliferation assay

The effects of OTS167 (OncoTherapy Science) on neuroblastoma cell proliferation *in vitro* were analyzed using the CellTiter 96 AQueous Non-radioactive Proliferation Assay kit (Promega). Cells were plated in triplicate wells in a 96-well plate and OTS167 was added 24 hours later at concentrations ranging from 0 to 1 uM. Following a 72 hour incubation, 3-(4,5-dimethylthiazol-2-yl)-5-(3-carboxymethoxyphenyl)-2-(4-sulfophenyl)-2H-tetrazolium (MTS) was added and absorbance measured using a Synergy 2 microplate reader (Bio-Tek Instruments). A nonlinear regression, sigmoidal four-parameter dose-response model was used to determine IC_{50} by plotting log of inhibitor concentration versus relative survival using Prism software (GraphPad). For synergy experiments, SK-N-BE2 and SK-N-DZ cells were plated as above and camptothecin (CPT, Alfa Aesar) and OTS167 were added alone or

in combination at concentrations from 0 to 2 uM. Following 48 hours incubation, MTS was added and absorbance measured as above. Combination Index (CI) was determined with CompuSyn Software using the Chou-Talalay method (23).

Clonogenic survival assay

SK-N-DZ and SK-N-BE2 were irradiated using a Philips RT250 Maxitron X-ray irradiator at 1.5 Gy/min and then plated at 5,000 or 2,000 cells per well respectively in 6-well plates containing complete medium with OTS167 or 0.5% DMSO vehicle control. Cultures were grown until colonies of > 50 cells had formed in the unirradiated DMSO vehicle control wells, 10 days for SK-N-DZ and 7 days for SK-N-BE2. SK-N-BE2 colonies were stained and imaged by washing each well once with PBS, staining and fixing with 0.5% crystal violet in 6% glutaraldehyde for 30 minutes, washing twice with water, drying, and imaging. The less-adherent SK-N-DZ colonies were stained by adding thiazolyl blue tetrazolium bromide (MTT) directly to the growth media to a final concentration of 0.05% and incubating the plates for 4 hours at 37 °C, 5% CO_2 before imaging. Automatic colony enumeration was performed using a custom set of macros for NIH ImageJ.

Western blot analysis

For the drug treatment studies, SK-N-BE2 and NMB cells were treated with indicated concentrations of OTS167 and/or CPT for 24 hours. For the radiation experiments, SK-N-BE2 cells were treated with 0, 2, or 4 Gy IR using a Philips RT250 Maxitron X-ray irradiator at 250 KVp and 15 mA with 1.0 mm Cu filter in 30/15×15 cm^2 cone, set at 10 cm from the sample with full backscatter. Indicated concentrations of OTS167 were added immediately after irradiation and incubated with cells for 24 hours. Protein lysates were prepared by boiling cell pellets in buffer containing 50 mM Tris-HCl pH 6.8, 2% SDS, and protease/phosphatase inhibitor cocktail (Sigma-Aldrich) for 5 minutes. Protein concentrations were determined with the BCA Protein Assay Reagent (Pierce). Ten ug of total protein were electrophoresed on Stain Free 4–20% SDS-PAGE gradient gels (BioRad) and transferred to nitrocellulose membranes (Amersham). Membranes were blocked in Tris Buffered Saline (TBS, pH 7.4) with 0.1% Tween-20 and 5% nonfat dry milk. Mouse EZH2 (Active Motif), rabbit pRPA32 (S4/S8) (Bethyl Laboratories), mouse RPA32 (Novus Biologicals), rabbit MYCN (Cell Signaling Technology), and mouse MYC (Santa Cruz) antibodies were used at a 1:1000 dilution. Mouse alpha tubulin antibody (Fitzgerald, 10R-T130A) was used at a 1:2000 dilution, mouse hsc70 (Invitrogen) and mouse anti-MELK (OncoTherapy Science) antibodies were used at a 1:10,000 dilution. Appropriate secondary antibodies were used and blots were developed with Clarity Western ECL Substrate (BioRad). Images were acquired on a BioRad ChemiDoc XRS+ imaging system and analyzed using Image Lab software. For quantitative image analyses all volumes were normalized by the total amount of protein in each sample determined by gel activation or by the levels of α-tubulin.

Cell cycle analysis

SK-N-BE2, NBL-W-N and NBL-W-S cells were treated with OTS167 from 0 to 8 nM for 24 hours, harvested and washed with cold Phosphate Buffered Saline (PBS, pH 7.4) followed by Accumax (Millipore) at room temperature for 10 minutes. The cells were pelleted at 1200

rpm for 5 minutes, washed with PBS, and 95% ethanol was added drop wise while vortexing, followed by 30 minutes incubation at −20°C. Before cytometric analysis cells were washed two more times with PBS and 1×10^6 cells were resuspended in 0.5 ml of Propidium Iodide/RNase Staining Buffer (BD). Cellular DNA content was then collected using a BD LSR II flow cytometer and analyzed using BD FACSDiva Software (BD).

Xenograft studies

To test the anti-tumor activity of OTS167 *in vivo*, female nude mice (Harlan) were subcutaneously injected with 1×10^7 SMS-KCNR neuroblastoma cells as previously described (22). Animals were randomized to treatment (n=9) or control groups (n=10) when tumors reached approximately 70 mm^3 and were palpable. The treatment group received 10 mg/kg OTS167 and control animals received vehicle alone. OTS167 or vehicle were injected intraperitoneally (IP) 2X/week for 3 weeks, tumor size was measured using a caliper, mice were weighed at time of measurement; and all animals were sacrificed 3 days after the last treatment. Tumors were resected, weighed, and parts of the tissue were snap frozen or fixed in formaldehyde and paraffin-embedded for pathologic evaluation. Tissue sections were stained with hematoxylin and eosin (H&E), Masson's trichrome, or anti-Ki67 antibody at the Pathology Core Facility at the University of Chicago. For the Minimal Residual Disease (MRD) model, when tumors reached 70 mm^3 mice were treated with 150 mg/kg cyclophosphamide (Baxter Healthcare) IP every other day for a total of 6 doses. Tumors were allowed to regress completely and the mice were randomized 5 days later to receive OTS167 (n=8) or vehicle control (n=8) 2X/week as above and treatment continued until tumor size reached 2000 mm^3. Animals were sacrificed and tumors removed as above. For injections, stock solutions of OTS167 were made up in DMSO and diluted in sterile 5% dextrose; cyclophosphamide was diluted in sterile water. All animal studies were conducted under protocol #71829 approved by the University of Chicago Institutional Animal Care and Use Committee.

Bioinformatics analysis

Publicly available microarray gene expression data for the Kocak dataset (709 patients, E-MTAB-1781) (24) and Versteeg dataset (88 patients, GSE16254) (25) were downloaded from EMBL and GEO, respectively. Raw microarray data were normalized within each cohort using the robust multi-array analysis algorithm to account for batch effects (26). MELK expression for downstream analysis was extracted using the A_23_P94422 probe for the Kocak dataset and the 204825_at probe for the Versteeg dataset. EZH2 expression was quantified using the A_23_P259641 probe from the Kocak dataset. Differences in MELK expression between binary groups was assessed by pairwise Mann-Whitney U and multiple groups by the Kruskal-Wallis method.

Survival analysis

Patients were categorized as having high or low expression of MELK using a sliding window to include at least ten percent of patients similar to prior reports (27). The log-rank test was used to calculate the p-value of the survival difference between high and low expression groups in each window. Multiple testing correction was done using the q-value

method (28) to account for the number of sliding windows. The most significant q-value for each analysis is reported.

Statistical analysis

All *in vitro* experiments were repeated at least three times in triplicate and standard deviations were calculated. All animal studies had at least five mice per group and mean values of the tumor volumes, weights, and vessel densities were compared. All quantitative values obtained in the experiments were evaluated using paired Student's t-test. A p-value of 0.05 was required to ascertain statistical significance. One way ANOVA was used to calculate differences in MELK and EZH2 protein levels across treatments with increasing concentrations of OTS167.

RESULTS

MELK expression in primary neuroblastoma tumors and cell lines

To investigate if high levels of MELK expression are associated with clinically aggressive neuroblastoma and poor outcome, we analyzed publicly available clinical and expression data in the Kocak dataset with 709 patients (E-MTAB-1781, Figure 1A, C, E, G), and the Versteeg cohort with 88 patients (GSE16254, Figure 1B, D, F). Survival was inferior for patients with high versus low levels of MELK expression in both cohorts (q-values $2.1e^{-14}$ and $2.4e^{-3}$, respectively). High expression of MELK was also significantly associated with advanced stage of disease ($p < 2.0e^{-16}$) and MYCN amplification ($p = 2.2e^{-16}$). Although risk group information was not available for the 88-patient cohort, increased levels of MELK expression were correlated with high-risk disease in the 709-patient cohort with p-value $2.2e^{-16}$ (Figure 1G). However, within the high-risk cohort, the level of MELK expression was not statistically significantly associated with outcome in the subset of 254 high-risk patients in the Kocak dataset after multiple testing correction.

We next measured MELK mRNA and protein expression in 11 neuroblastoma cell lines by qPCR and Western blot analysis. MELK was detected in all of the cell lines, although the levels of expression varied (Figure 2). High levels of MELK protein were observed in neuronal N-type cell lines. N-type cells express neuronal markers of differentiation, commonly have neurite extension when cultured on plastic, generally express high levels of MYCN, and form tumors in nude mice (29). We show that high levels of MYCN are expressed in all of N-type cell lines we analyzed with the exception of SH-SY5Y, which expresses high levels of MYC (Supplementary Figure 1). In contrast, low levels of MELK were detected in the S-type cell lines. These substrate adherent cells, do not express neuronal markers but may express Glial Fibrillary Acidic Protein, and generally are not tumorigenic *in vivo* (29). Although MELK protein levels were higher in the tumorigenic N-type cell lines, MELK mRNA levels were more variable, suggesting that MELK may be additionally regulated at the level of translation and/or protein stability.

OTS167 inhibits growth of neuroblastoma cells that express high levels of MELK

The effects of OTS167 on cell growth were evaluated in 11 neuroblastoma cell lines. The IC_{50} was less than 9 nM for all tested N-type tumorigenic cell lines (Figure 3A, B). In

contrast, the non-tumorigenic S-type cells have low levels of MELK expression and were more resistant to OTS167 with IC_{50} ranging from 25 to 44 nM. Thus, similar to the adult cancers, low nM concentrations of OTS167 inhibited proliferation of neuroblastoma cells with high MELK expression.

We also measured the effects of OTS167 on cell cycle in the N-type SK-N-BE2 cell line and N/S-type pair NBL-W-N and NBL-W-S. For this analysis, cells were exposed to OTS167 for 24 hours at concentrations below the IC_{50} to prevent cytotoxicity and cell death. In both N-type cell lines, SK-N-BE2 and NBL-W-N, a decrease in the number of cells in G1 phase and increase in the number of cells in S phase was observed, which reached statistical significance at 8 nM concentrations of OTS167. We also observed an increased number of cells in Sub-G1 phase at this concentration of OTS167, although statistical significance was not achieved (Figure 3C). Although OTS167 induced similar changes in the cell cycle in S-type NBL-W-S cells, statistical significance was not reached and no increase in the number of cells in Sub-G1 phase was observed. Thus, similar to previous studies in acute myeloid leukemia cells (7), the progression of mitosis is inhibited by OTS167 in neuroblastoma cells.

OTS167 inhibits the growth of neuroblastoma xenografts

Intraperitoneal administration of 10 mg/kg of OTS167 twice per week also significantly inhibited the growth of neuroblastoma xenografts comprised of N-type SMS-KCNR cells (Figure 4A). Animals were sacrificed after three weeks of treatment, and the average weight of the OTS167-treated tumors was significantly decreased compared to controls (0.45±0.21 g versus 2.00±0.57 g; $p<0.05$) (Figure 4B, C). Histologic examination of H&E stained sections revealed large areas of hemorrhage in the control tumors, whereas little to no hemorrhage was detected in the tumors treated with OTS167 (Figure 4D). Masson's trichrome staining showed large areas of interstitial stroma with abundant depositions of extracellular matrix (ECM) in treated tumors, while control tumors where comprised almost exclusively of neoplastic cells (Figure 4E). To detect proliferating neoplastic cells, xenograft sections were stained for Ki67. No difference in the intensity of staining was observed between control and treated sections (Figure 4F).

OTS167 activity in an MRD model

To investigate the activity of OTS167 in the setting of MRD, we treated mice with this MELK inhibitor after chemotherapy-induced tumor regression. Mice with palpable neuroblastoma xenografts first were treated with cyclophosphamide. Following tumor regression, the mice were randomized to receive either 10 mg/kg of OTS167 or control vehicle, twice per week as above until tumor size reached 2000 mm^3. Although all mice treated with cyclophosphamide followed by OTS167 or vehicle eventually developed recurrent tumors, prolonged survival was seen in the cohort treated with OTS167 (104±10 days versus 80±12 days; $p=0.01$, Figure 4G). Furthermore, the average tumor volume was significantly decreased in the animals treated with OTS167 from day 65 until day 72 ($p<0.05$, Figure 4H).

OTS167 down-regulates MELK and EZH2

To investigate if OTS167 directly modifies MELK expression in neuroblastoma, we measured MELK protein levels by Western blot analysis after 24 hours of treatment. Comparison of control versus treated cells, demonstrated that OTS167 statistically significantly decreased the quantity of MELK protein in SK-N-BE2, NMB, and SMS-KCNR neuroblastoma cell lines ($p=3.18e^{-06}$, 0.000481 and 0.00902, respectively, Figure 5A, B). We next evaluated the effects of OTS167 on EZH2, a known MELK target (11), by Western blot, and found that EZH2 protein levels were also significantly decreased in SK-N-BE2, NMB, and SMS-KCNR cells with treatment ($p=2.55e^{-05}$, $2.53e^{-09}$, and 0.00587, respectively, Figure 5A - C). Analysis of the Kocak expression data shows that the levels of MELK and EZH2 mRNA are highly correlated in primary tumors (Pearson's r = 0.68, Figure 5D), further supporting a role for MELK in the regulation of EZH2 in neuroblastoma. Interestingly, OTS167 treatment did not result in a decrease in MELK and EZH2 transcript levels in SK-N-BE2 cells (Supplementary Figure 2B). Thus, OTS167-mediated post-translational modifications may regulate MELK and EZH2 protein in neuroblastoma.

OTS167 increases sensitivity to CPT and radiation

MELK inhibition has been reported to increase sensitivity to chemotherapy and radiation in adult cancers (3,9–11). To investigate if sensitivity to the DNA damaging agent CPT is also increased in neuroblastoma cells when MELK is inhibited with OTS167, we tested both drugs for synergy using a constant dilution ratio to determine drug CI (23). With this method a CI > 1 indicates there is drug antagonism; a CI=1 indicates the combination therapy is additive; and a CI < 1 indicates there is a synergistic interaction between the drugs. We analyzed the CI for OTS167 and CPT in SK-N-DZ and SK-N-BE2 cells and found that in both cell lines the drugs were synergistic at concentrations ranging from 3.125 nM to 250 nM (Figure 6A). To investigate if the sensitivity to radiation therapy is also increased by OTS167, clonogenic survival assays were performed which demonstrated that OTS167 and radiation exerted supra-additive lethal effects in both neuroblastoma cell lines (Figure 6B).

To investigate the mechanisms by which OTS167 treatment enhances sensitivity to CPT, we measured phosphorylation of serine 4 and 8 of Replication Protein A2 (RPA32), a marker of collapsed replication forks, in neuroblastoma cells treated with CPT alone or in combination with OTS167. Phosphorylation of the 32kDa subunit of RPA32 was increased in neuroblastoma cells following treatment with CPT, indicative of the expected increase in formation of collapsed replication forks. Co-treatment of neuroblastoma cells with CPT plus OTS167 resulted in a reduction in collapsed replication forks, and it significantly decreased RPA32 phosphorylation with 10–50 nM concentrations of OTS167 ($p < 0.05$, Figure 6C). Similar results were observed in NBL-W-N and NBL-W-S cells (Supplementary Figure 3). In experiments using radiation in the place of CPT, treatment with 10 nM and 50 nM OTS167 also significantly reduced RPA32 phosphorylation in a dose dependent manner ($p < 0.05$, Figure 6D). These results suggest that MELK inhibition with OTS167 attenuates the processing of stressed replication forks into frank double-stranded breaks, thereby interfering with the normal processing of these genotoxic lesions, which in turn sensitizes neuroblastoma cells to radiation and CPT.

DISCUSSION

MELK is known to promote oncogenic growth in common adult malignancies, but its role in neuroblastoma pathogenesis remains largely unknown. In this study, we analyzed publicly available clinical and expression data and demonstrated that high levels of MELK expression in primary neuroblastomas were significantly associated with high-risk disease and poor outcome. We also found that MELK expression associates with the phenotype of neuroblastoma cells, with high levels of MELK detected in N-type neuroblastoma cell lines that are capable of forming tumors in nude mice, whereas lower levels were present in S-type cell lines that are not tumorigenic. Pharmacologic inhibition of MELK with OTS167 decreased the growth of neuroblastoma cells. Similar to adult cancer studies, we found that the sensitivity to OTS167 was increased in the cell lines with high MELK expression. We also show that OTS167 suppressed the growth of neuroblastoma xenografts. Taken together, these results indicate that MELK may be a clinically relevant therapeutic target in neuroblastoma, and that the level of MELK expression may serve as a biomarker for response to OTS167.

We also tested OTS167 in a neuroblastoma mouse model of MRD. In patients with neuroblastoma, MRD is not detected by standard tumor evaluation tests and commonly persists following consolidation with myeloablative chemotherapy and stem cell transplant, eventually leading to relapse. In an effort to eliminate refractory microscopic disease, post-consolidation therapy is now part of standard treatment of high-risk neuroblastoma, and survival has been improved following the incorporation of isotretinoin and immunotherapy in this setting (30). There is increasing evidence that neuroblastoma stem cells or tumor initiating cells are resistant to therapy and persist following treatment. Because MELK is important in the maintenance of tumor stem cells (9,12,31), we hypothesized that OTS167 may be effective in the setting of MRD. Our studies show that OTS167 treatment delayed relapse and prolonged survival of the animals with MRD following treatment with cyclophosphamide. However, tumor recurrence was observed in all of the mice, indicating that OTS167 alone was not sufficient to eliminate the residual neuroblastoma cells.

Our results confirm and expand the studies recently published by Guan and co-workers showing significant associations between high levels of MELK expression and poor survival in patients with neuroblastoma (18). These investigators also demonstrated that MYCN directly regulates MELK transcription, and they reported that the levels of MELK expression were statistically significantly higher in tumors with MYCN amplification. Although there was overlap of the datasets analyzed in the two studies, we evaluated an extended Kocak dataset containing expression data and clinical information for 709 patients and also analyzed an independent Versteeg dataset with 88 patients. We detected significantly higher levels of MELK in high-risk patients compared to the non-high-risk cohort. Among the high-risk subset of 254 patients, there was a trend associating inferior event-free survival with increased levels of MELK expression, although statistical significance was not met. In concert with our results, Guan and colleagues also demonstrated that OTS167 significantly inhibited neuroblastoma cell proliferation, blocked cell cycle progression, and suppressed the growth of neuroblastoma xenografts. While many of neuroblastoma cell lines evaluated in their study were different than the ones used in our

study, SH-SY5Y was tested in both studies. In both studies, the growth of this MYCN-non-amplified cell line was suppressed with MELK inhibition, suggesting that this treatment strategy may be effective in neuroblastoma tumors with or without MYCN amplification. In the Guan study, 208 nM of OTS 167 was required to achieve the IC_{50}, while in our study the IC_{50} for SH-SY5Y was 2.2 nM. The reason for these disparities in OTS167 sensitivity are not clear, but may be related to differences in the drugs, which were obtained from different manufacturers, or experimental conditions of cell culture.

The mechanisms by which MELK promotes cancer growth remain largely unknown. Studies in glioma have shown that MELK phosphorylates and forms a complex with FoxM1, a transcription factor which functions as an oncogene and regulator of stem-like properties (12). This complex activates EZH2, a lysine methyltransferase which catalyzes trimethylation of histone 3 at lysine 27, leading to inhibited transcription of genes involved in differentiation (11). Our studies suggest that MELK-dependent EZH2 signaling also occurs in neuroblastoma, as OTS167 treatment down-regulated the protein levels of both MELK and EZH2. However, MELK and EZH2 RNA levels were not decreased in neuroblastoma cells with OTS167 treatment, indicating that the changes in MELK and EZH2 protein observed in neuroblastoma cells treated with OTS167 were not transcriptionally regulated. Rather, OTS167 may mediate post-translational modifications that result in the down-regulated expression of MELK and EZH2 protein in neuroblastoma. Indeed, in breast cancer, another small molecule inhibitor MELK-T1 has been shown to inhibit MELK autophosphorylation, leading to proteasomal degradation (32). In medulloblastoma MELK directly binds and phosphorylates EZH2 (33). Although MYCN has been shown to regulate EZH2 (34,35), significant correlations between MYCN and EZH2 expression in the neuroblastoma cell lines we analyzed were not detected. We also did not detect significant associations between MYCN and EZH2 expression the in primary tumors analyzed in the R2 database (http://r2.amc.nl). Further studies will be required to clarify the interactions between MYCN, EZH2, and MELK in neuroblastoma.

MELK-dependent EZH2 signaling has been reported to be associated with therapy resistance in adult cancers. In glioblastoma cells, both MELK and EZH2 are up-regulated with radiation treatment and higher levels of both proteins are present in relapsed glioblastoma compared to diagnostic tumors (11). MELK has also been identified as a biomarker of radioresistance in breast cancer. Higher levels of MELK are detected in clinically aggressive, therapy-resistant triple-negative breast cancer and therapy resistant triple-negative breast cancer cell lines (32). Further, increased sensitivity to radiation following pharmacologic or genomic inhibition of MELK has been reported in several adult cancer models (3,9,10,32). In our studies, a synergistic response was observed in neuroblastoma cells treated with OTS167 and CPT or radiation, suggesting that MELK-dependent EZH2 signaling inhibition also sensitizes neuroblastoma to at least these DNA damaging agents.

Although the mechanisms responsible for the enhanced sensitivity to radiation and chemotherapy with MELK inhibition are not completely understood, EZH2 plays a recently discovered role in processing stalled replication forks into double stand DNA breaks (DSB). This involves recruitment of the MUS81 nuclease, which generates DSB that that can serve

as a substrate for homologous recombination (HR) DNA repair (36). This suggests that MELK inhibition may sensitize cells to radiation and CPT by interfering with the normal processing of stalled replication forks into DSB intermediates that serve as HR substrates (see model in Figure 6E). We tested this hypothesis by treating neuroblastoma cells with either radiation or CPT. While radiation is commonly used to experimentally generate immediate DSBs, it also produces clustered patterns of oxidative damage of bases and sugars that can impair DNA replication (37). Consistent with this pattern of damage, radiation exposure results in secondary replication-induced DSBs that appear at relatively late time points (7–9 hours post-irradiation) and are repaired by HR (38). Phosphorylation of the 32kDa subunit of RPA32 was detected in neuroblastoma cells treated with radiation, indicative of the expected collapsed replication forks. In support of our hypothesis, OTS167 attenuated radiation-induced RPA32 phosphorylation. We additionally investigated this hypothesis using the topoisomerase I inhibitor CPT, which produces replication-associated DSBs that are generated by the Mus81-Eme1 endonuclease. These endonuclease-induced DSBs play an important role in dissipating the excessive supercoiling resulting from topoisomerase I inhibition, and this process ultimately aids in replication fork progression and improved cell survival (39). As expected, treatment of the neuroblastoma cells with CPT resulted in the formation of collapsed replication forks, again quantified as a function of phosphorylation of the 32kDa subunit of RPA32. However, co-treatment with OTS167 antagonized the formation of collapsed replication forks after treatment with either CPT or radiation, supporting our proposed mechanism of action wherein MELK indirectly mediates the processing of replication-blocking lesions into DSBs that are suitable substrates for HR-mediated repair.

Taken together, our results indicate that MELK is a therapeutic target in neuroblastoma and provide the rationale for testing OTS167 in clinical trials for children with high-risk disease. By also inhibiting EZH2, OTS167 modifies processing of DNA lesions and increases sensitivity to radiation and CPT. Further studies testing the activity of OTS167 combined with other chemotherapeutic agents, radiation, and/or targeted radiopharmaceuticals such as ^{131}I-meta-iodobenzylguanidine (MIBG) may lead to the development of novel therapeutic strategies that will prove to be effective in the treatment of patients with high-risk neuroblastoma.

Supplementary Material

Refer to Web version on PubMed Central for supplementary material.

Acknowledgements

This work was supported in part by Hyundai Hope on Wheels (SLC), Neuroblastoma Children's Cancer Society (SLC), the Children's Neuroblastoma Cancer Foundation (SLC), the Matthew Bittker Foundation (SLC), and the Elise Anderson Neuroblastoma Research Fund (SLC), Conquer Cancer Foundation (MAA), Cancer Research Foundation (MAA) and the Cancer Center Support Grant P30CA014599. Also supported by the National Institutes of Health grants K12CA139160 (MAA), K08CA226237 (MAA), and 2R01CA142642 (PPC). The contents are solely the responsibility of the authors and do not necessarily represent the official views of the NIH.

Financial Support: Hyundai Hope on Wheels (SLC), Neuroblastoma Children's Cancer Society (SLC), the Children's Neuroblastoma Cancer Foundation (SLC), the Matthew Bittker Foundation (SLC), the Elise Anderson Neuroblastoma Research Fund (SLC), Conquer Cancer Foundation (MAA), Cancer Research Foundation (MAA),

and the Cancer Center Support Grant P30CA014599. Also supported by the National Institutes of Health grants K12CA139160 (MAA), K08CA226237 (MAA), and 2R01CA142642 (PPC).

REFERENCES

1. Pinto NR, Applebaum MA, Volchenboum SL, Matthay KK, London WB, Ambros PF, et al. Advances in Risk Classification and Treatment Strategies for Neuroblastoma. J Clin Oncol 2015;33(27):3008–17. [PubMed: 26304901]
2. Applebaum MA, Henderson TO, Lee SM, Pinto N, Volchenboum SL, Cohn SL. Second malignancies in patients with neuroblastoma: the effects of risk-based therapy. Pediatr Blood Cancer 2015; 62(1):128–33. [PubMed: 25251613]
3. Ganguly R, Mohyeldin A, Thiel J, Kornblum HI, Beullens M, Nakano I. MELK - a conserved kinase: functions, signaling, cancer, and controversy. Clin Transl Med 2015;4:11. [PubMed: 25852826]
4. Jiang P, Zhang D. Maternal Embryonic Leucine Zipper Kinase (MELK): a novel regulator in cell cycle control, embryonic development, and cancer. Int J Mol Sci 2013;14(11):21551–60. [PubMed: 24185907]
5. Kohler RS, Kettelhack H, Knipprath-Meszaros AM, Fedier A, Schoetzau A, Jacob F, et al. MELK expression in ovarian cancer correlates with poor outcome and its inhibition by OTSSP167 abrogates proliferation and viability of ovarian cancer cells. Gynecol Oncol 2017;145(1):159–66. [PubMed: 28214016]
6. Inoue H, Kato T, Olugbile S, Tamura K, Chung S, Miyamoto T, et al. Effective growth-suppressive activity of Maternal Embryonic Leucine-Zipper Kinase (MELK) inhibitor against small cell lung cancer. Oncotarget 2016;7(12):13621–33. [PubMed: 26871945]
7. Alachkar H, Mutonga MB, Metzeler KH, Fulton N, Malnassy G, Herold T, et al. Preclinical efficacy of Maternal Embryonic Leucine-Zipper Kinase (MELK) inhibition in acute myeloid leukemia. Oncotarget 2014;5(23):12371–82. [PubMed: 25365263]
8. Li S, Li Z, Guo T, Xing XF, Cheng X, Du H, et al. Maternal Embryonic Leucine Zipper Kinase serves as a poor prognosis marker and therapeutic target in gastric cancer. Oncotarget 2016;7(5): 6266–80. [PubMed: 26701722]
9. Gu C, Banasavadi-Siddegowda YK, Joshi K, Nakamura Y, Kurt H, Gupta S, et al. Tumor-specific activation of the C-JUN/MELK pathway regulates glioma stem cell growth in a p53-dependent manner. Stem cells 2013;31(5):870–81. [PubMed: 23339114]
10. Speers C, Zhao SG, Kothari V, Santola A, Liu M, Wilder-Romans K, et al. Maternal Embryonic Leucine Zipper Kinase (MELK) as a novel mediator and biomarker of radioresistance in human breast cancer. Clin Cancer Res 2016;22(23):5864–75. [PubMed: 27225691]
11. Kim SH, Joshi K, Ezhilarasan R, Myers TR, Siu J, Gu C, et al. EZH2 protects glioma stem cells from radiation-induced cell death in a MELK/FOXM1-dependent manner. Stem Cell Reports 2015;4(2):226–38. [PubMed: 25601206]
12. Joshi K, Banasavadi-Siddegowda Y, Mo X, Kim SH, Mao P, Kig C, et al. MELK-dependent FOXM1 phosphorylation is essential for proliferation of glioma stem cells. Stem Cells 2013;31(6): 1051–63. [PubMed: 23404835]
13. Chung S, Suzuki H, Miyamoto T, Takamatsu N, Tatsuguchi A, Ueda K, et al. Development of an orally-administrative MELK-targeting inhibitor that suppresses the growth of various types of human cancer. Oncotarget 2012;3(12):1629–40. [PubMed: 23283305]
14. Kato T, Inoue H, Imoto S, Tamada Y, Miyamoto T, Matsuo Y, et al. Oncogenic roles of TOPK and MELK, and effective growth suppression by small molecular inhibitors in kidney cancer cells. Oncotarget 2016;7(14):17652–64. [PubMed: 26933922]
15. Stefka AT, Park JH, Matsuo Y, Chung S, Nakamura Y, Jakubowiak AJ, et al. Anti-myeloma activity of MELK inhibitor OTS167: effects on drug-resistant myeloma cells and putative myeloma stem cell replenishment of malignant plasma cells. Blood Cancer J 2016;6(8):e460. [PubMed: 27540718]
16. Arend KC, Lenarcic EM, Vincent HA, Rashid N, Lazear E, McDonald IM, et al. Kinome profiling identifies druggable targets for novel Human Cytomegalovirus (HCMV) antivirals. Mol Cell Proteomics 2017;16(4 suppl 1):S263–S76. [PubMed: 28237943]

17. Wang Y, Lee YM, Baitsch L, Huang A, Xiang Y, Tong H, et al. MELK is an oncogenic kinase essential for mitotic progression in basal-like breast cancer cells. Elife 2014;3:e01763. [PubMed: 24844244]
18. Guan S, Lu J, Zhao Y, Yu Y, Li H, Chen Z, et al. MELK is a novel therapeutic target in high-risk neuroblastoma. Oncotarget 2018;9(2):2591–602. [PubMed: 29416794]
19. Matsuda T, Kato T, Kiyotani K, Tarhan YE, Saloura V, Chung S, et al. p53-independent p21 induction by MELK inhibition. Oncotarget 2017;8(35):57938–47. [PubMed: 28938528]
20. Cohn SL, Salwen H, Quasney MW, Ikegaki N, Cowan JM, Herst CV, et al. Prolonged N-Myc protein half-life in a neuroblastoma cell line lacking N-Myc amplification. Oncogene 1990;5(12): 1821–7. [PubMed: 2284101]
21. Foley J, Cohn SL, Salwen HR, Chagnovich D, Cowan J, Mason KL, et al. Differential expression of N-Myc in phenotypically distinct subclones of a human neuroblastoma cell line. Cancer Res 1991;51(23 Pt 1):6338–45. [PubMed: 1933896]
22. Chlenski A, Liu S, Crawford SE, Volpert OV, DeVries GH, Evangelista A, et al. SPARC is a key Schwannian-derived inhibitor controlling neuroblastoma tumor angiogenesis. Cancer Res 2002;62(24):7357–63. [PubMed: 12499280]
23. Chou TC. Drug combination studies and their synergy quantification using the Chou-Talalay method. Cancer Res 2010;70(2):440–6. [PubMed: 20068163]
24. Oberthuer A, Juraeva D, Hero B, Volland R, Sterz C, Schmidt R, et al. Revised risk estimation and treatment stratification of low- and intermediate-risk neuroblastoma patients by integrating clinical and molecular prognostic markers. Clin Cancer Res 2015;21(8):1904–15. [PubMed: 25231397]
25. Molenaar JJ, Domingo-Fernandez R, Ebus ME, Lindner S, Koster J, Drabek K, et al. LIN28B induces neuroblastoma and enhances MYCN levels via let-7 suppression. Nature genetics 2012;44(11):1199–206. [PubMed: 23042116]
26. Irizarry RA, Hobbs B, Collin F, Beazer-Barclay YD, Antonellis KJ, Scherf U, et al. Exploration, normalization, and summaries of high density oligonucleotide array probe level data. Biostatistics 2003;4(2):249–64. [PubMed: 12925520]
27. Applebaum MA, Jha AR, Kao C, Hernandez KM, DeWane G, Salwen HR, et al. Integrative genomics reveals hypoxia inducible genes that are associated with a poor prognosis in neuroblastoma patients. Oncotarget 2016;7(47):76816–26. [PubMed: 27765905]
28. Storey JD. A direct approach to false discovery rates. J Roy Stat Soc B 2002;64:479–98.
29. Thiele CJ. Neuroblastoma Cell Lines In: Masters J, editor. Neuroblastoma. Volume 1 Lancaster, UK: Kluwer Academic Publishers; 1998p 21–53.
30. Applebaum MA, Desai AV, Glade Bender JL, Cohn SL. Emerging and investigational therapies for neuroblastoma. Expert Opin Orphan Drugs 2017;5(4):355–68. [PubMed: 29062613]
31. Nakano I, Masterman-Smith M, Saigusa K, Paucar AA, Horvath S, Shoemaker L, et al. Maternal Embryonic Leucine Zipper Kinase is a key regulator of the proliferation of malignant brain tumors, including brain tumor stem cells. J Neurosci Res 2008;86(1):48–60. [PubMed: 17722061]
32. Beke L, Kig C, Linders JT, Boens S, Boeckx A, van Heerde E, et al. MELK-T1, a small-molecule inhibitor of protein kinase MELK, decreases DNA-damage tolerance in proliferating cancer cells. Biosci Rep 2015;35(6):e00267. [PubMed: 26431963]
33. Liu H, Sun Q, Sun Y, Zhang J, Yuan H, Pang S, et al. MELK and EZH2 Cooperate to regulate medulloblastoma cancer stem-like cell proliferation and differentiation. Mol Cancer Res 2017;15(9):1275–86. [PubMed: 28536141]
34. He S, Liu Z, Oh DY, Thiele CJ. MYCN and the epigenome. Front Oncol 2013;3:1. [PubMed: 23373009]
35. Corvetta D, Chayka O, Gherardi S, D'Acunto CW, Cantilena S, Valli E, et al. Physical interaction between MYCN oncogene and Polycomb Repressive Complex 2 (PRC2) in neuroblastoma: functional and therapeutic implications. J Biol Chem 2013;288(12):8332–41. [PubMed: 23362253]
36. Rondinelli B, Gogola E, Yucel H, Duarte AA, van de Ven M, van der Sluijs R, et al. EZH2 promotes degradation of stalled replication forks by recruiting MUS81 through histone H3 trimethylation. Nat Cell Biol 2017;19(11):1371–8. [PubMed: 29035360]

37. Leadon SA. Repair of DNA damage produced by ionizing radiation: A Minireview. Semin Radiat Oncol 1996;6(4):295–305. [PubMed: 10717187]

38. Groth P, Orta ML, Elvers I, Majumder MM, Lagerqvist A, Helleday T. Homologous recombination repairs secondary replication induced DNA double-strand breaks after ionizing radiation. Nucleic Acids Res 2012;40(14):6585–94. [PubMed: 22505579]

39. Regairaz M, Zhang YW, Fu H, Agama KK, Tata N, Agrawal S, et al. Mus81-mediated DNA cleavage resolves replication forks stalled by topoisomerase I-DNA complexes. J Cell Biol 2011;195(5):739–49. [PubMed: 22123861]

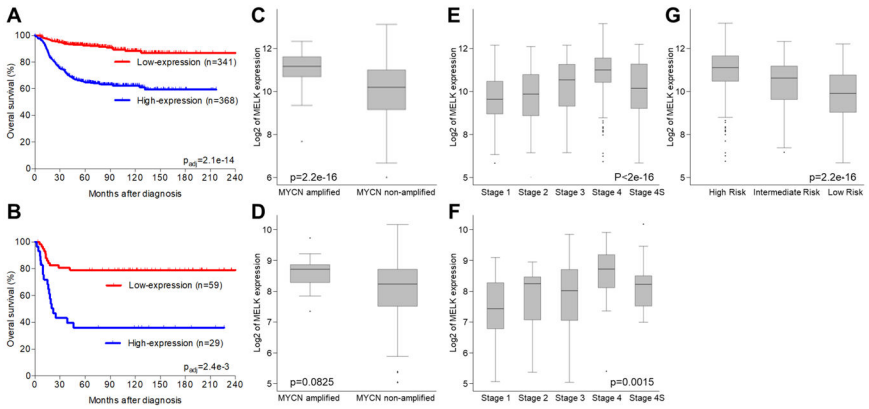

Figure 1. MELK expression correlates with survival, established prognostic markers, and risk-group in neuroblastoma.

Kaplan-Meier survival analysis in 2 cohorts with 709 (**A**) and 88 (**B**) annotated neuroblastoma tumors demonstrated that high levels of MELK expression (shown in blue) are associated with clinically aggressive disease and worse overall survival. In both cohorts higher expression of MELK was significantly associated with MYCN amplification (**C,D**) and higher stage (**E,F**), respectively. High MELK expression was also associated with high risk disease in a cohort of 709 patients (**G**). Risk information was not available for the cohort of 88 patients.

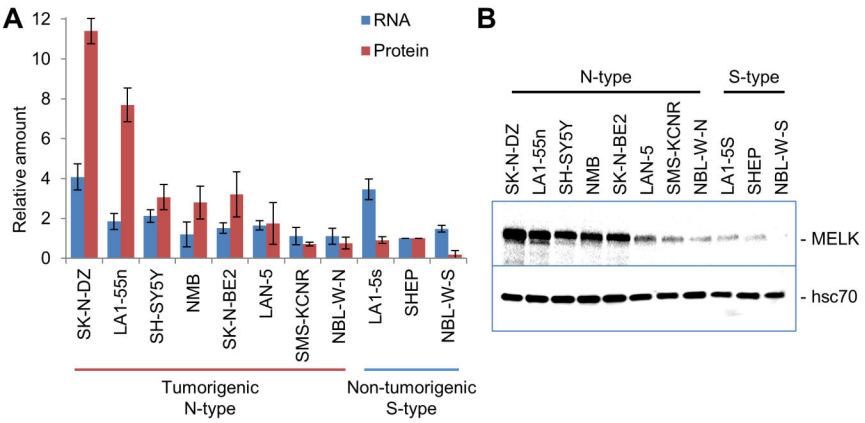

Figure 2. MELK is expressed at higher levels in tumorigenic, neuronal N-type neuroblastoma cells compared to non-tumorigenic, substrate-adherent S-type neuroblastoma cells.

A. qPCR and Western blot analyses show that MELK mRNA and protein were detected in all neuroblastoma cell lines. Although mRNA expression was comparable in all cell lines, levels of MELK protein were higher in a majority of the tumorigenic N-type cells. To allow for comparison between different experiments, both mRNA and protein expression were normalized to levels in SHEP cells. **B.** Representative image of Western blot.

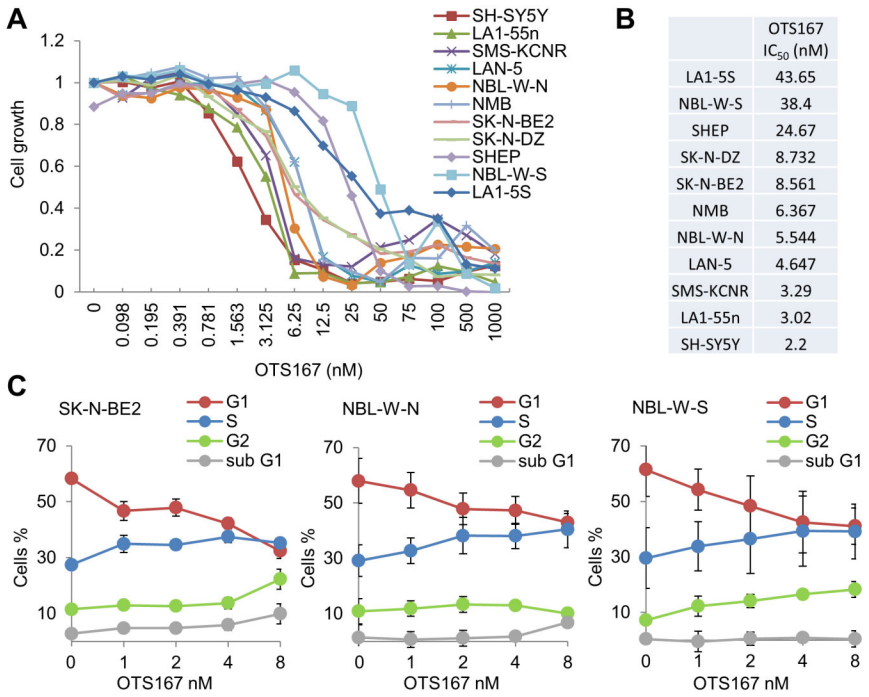

	OTS167 IC_{50} (nM)
LA1-5S	43.65
NBL-W-S	38.4
SHEP	24.67
SK-N-DZ	8.732
SK-N-BE2	8.561
NMB	6.367
NBL-W-N	5.544
LAN-5	4.647
SMS-KCNR	3.29
LA1-55n	3.02
SH-SY5Y	2.2

Figure 3. OTS167 inhibits cell cycle progression and neuroblastoma growth *in vitro.*

A. Representative proliferation assay of 11 neuroblastoma cell lines after 72 hour incubation with increasing concentrations of OTS167. **B.** Average IC_{50} determined in at least 3 independent experiments. An IC_{50} of less than 9 nM was observed in eight N-type cell lines. Non-tumorigenic S-type cells were more resistant to drug, which further indicated that MELK promotes tumorigenicity in neuroblastoma. **C.** Cell cycle analysis showed that treatment with OTS167 impaired mitosis progression of SK-N-BE2, NBL-W-N, and NBL-W-S cells.

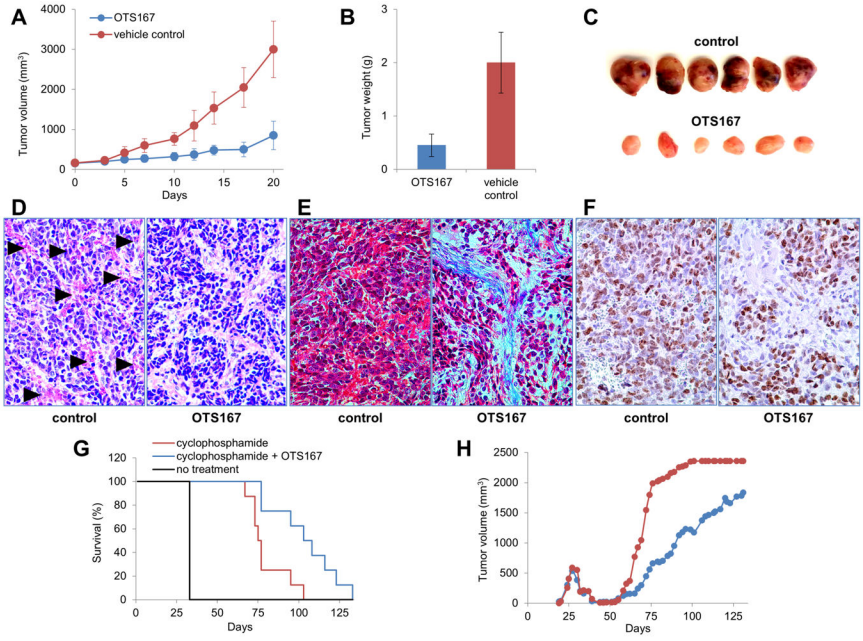

Figure 4. OTS167 suppresses the growth of neuroblastoma xenografts

A. Tumor size during treatment. OTS167 significantly suppressed neuroblastoma progression ($p<0001$). **B.** Tumor weight at the endpoint. The average weight of the OTS167-treated tumors at the end of the treatment was 77% lower than the average weight of the control tumors ($p<0.05$). **C.** Representative tumors. Control tumors appeared more hemorrhagic than tumors treated with OTS167. **D.** Representative tumor sections stained with H&E. Hemorrhage (arrowheads) is evident in control tumors but is not observed in the OTS167-treated tumors. Magnification x200. **E.** Representative tumor sections stained with Masson's trichrome. Control tumors were comprised mostly of neoplastic cells which appear red. Tumors treated with OTS167 had significantly more stromal cells and depositions of ECM, stained blue. Magnification x400. **F.** Representative tumor sections stained with anti-Ki67 antibody. Magnification x400. **G.** OTS167 prolongs survival in the setting of MRD. Animals with xenografted neuroblastoma tumors were treated with cyclophosphamide until remission. Treatment with OTS167 was started when no visible tumors were present, mice in the control group were treated with vehicle. Animals were sacrificed when size of relapsed tumors reached 2000 mm^3. Treatment with OTS167 delayed relapse and prolonged survival from 80±12 days in the control group to 104±10 days in the group treated with OTS167 ($p=0.01$). **H.** The average tumor volume was significantly decreased in the animals treated with OTS167 (blue circles) from day 65 until day 72 compared to the control group (red circles, $p<0.05$).

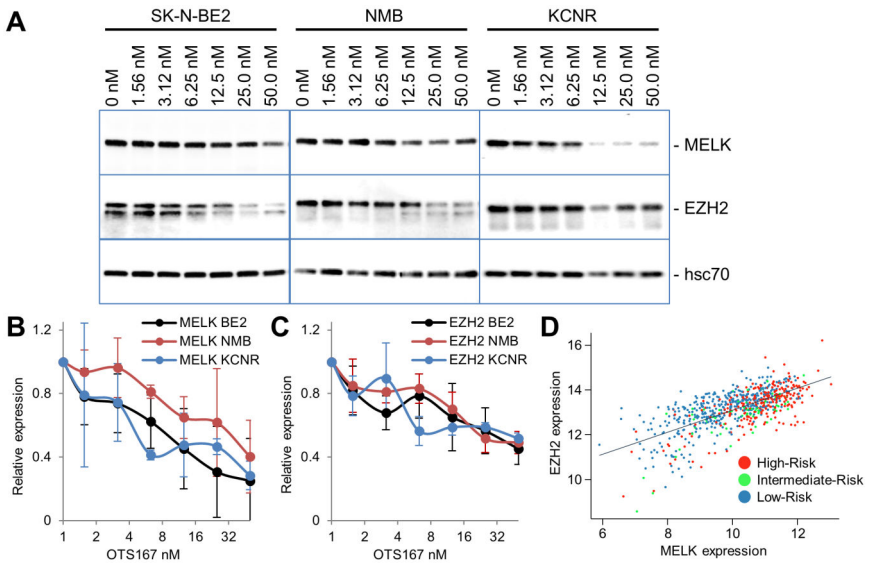

Figure 5. OTS167 down-regulates MELK and EZH2.

A. Western blot shows downregulation of protein levels of MELK and EZH2 after treatment of neuroblastoma cell lines SK-N-BE2, NMB, and SMS-KCNR with indicated concentrations of OTS167 for 24 hours. **B, C.** Relative average quantities ±SD of MELK and EZH2 proteins determined in at least 3 independent experiments. Downregulation was statistically significant by one way ANOVA in all treatments. **D.** Correlation between MELK and EZH2 expression in neuroblastoma patients (Pearson's r=0.68).

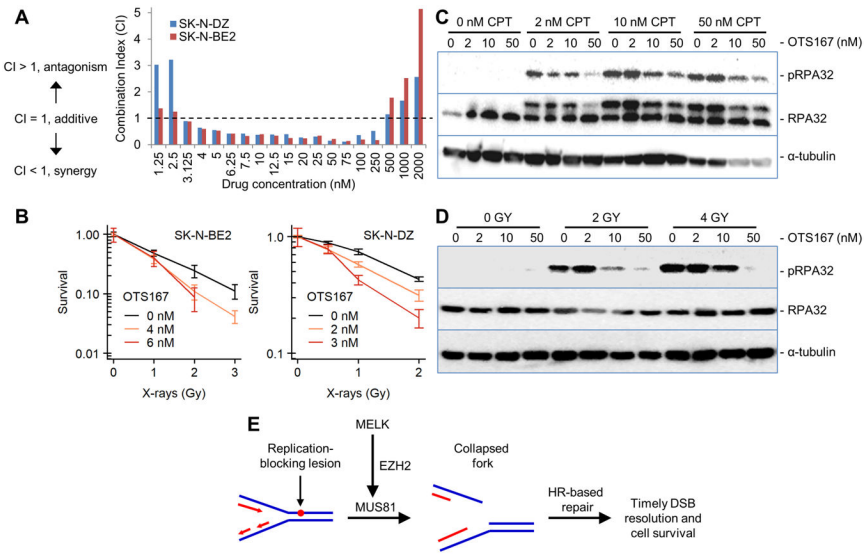

Figure 6. OTS167 sensitizes neuroblastoma cells to CPT and IR.

A. Synergy between OTS167 and CPT was determined *in vitro* in SK-N-DZ and SK-N-BE2 cells. Using the Chou-Talai method, synergistic CI values below 1 were observed for concentrations of each drug from 3 to 250 nM. **B.** Clonogenic survival assay showing that OTS167 sensitizes neuroblastoma cells to radiation. Error bars denote the standard error for three replicates. **C.** Western blot analysis quantifying total RPA32 and RPA32 phosphorylation in SK-N-BE2 cells following treatment with CPT alone or CPT combined with OTS167. **D.** Western blot analysis quantifying total RPA32 and RPA32 phosphorylation in SK-N-BE2 cells following treatment with IR alone or IR combined withOTS167. **E.** Schematic of proposed role for MELK in processing stalled replication forks thereby promoting timely DSB resolution and cell survival.